THE JOURNAL OF IMMUNOLOGY

Dermal Regulatory T Cells Display Distinct Migratory Behavior That Is Modulated during Adaptive and Innate Inflammation

Zachary Chow, Scott N. Mueller, James A. Deane and Michael J. Hickey

J Immunol published online 12 August 2013
http://www.jimmunol.org/content/early/2013/08/10/jimmunol.1203205

The Journal of Immunology is published twice each month by The American Association of Immunologists, Inc., 9650 Rockville Pike, Bethesda, MD 20814-3994.

Print ISSN: 0022-1767 Online ISSN: 1550-6606.

Published August 12, 2013, doi:10.4049/jimmunol.1203205

Dermal Regulatory T Cells Display Distinct Migratory Behavior That Is Modulated during Adaptive and Innate Inflammation

Zachary Chow,* Scott N. Mueller,† James A. Deane,*,[1] and Michael J. Hickey*,[1]

Regulatory T cells (Tregs) are important in controlling skin inflammation, an effect dependent on their ability to home to this organ. However, little is known regarding their behavior in the skin. In this study, we used multiphoton imaging in Foxp3-GFP mice to examine the behavior of endogenous Tregs in resting and inflamed skin. Although Tregs were readily detectable in the uninflamed dermis, most were nonmotile. Induction of contact sensitivity increased the proportion of motile Tregs, and also induced Treg recruitment. This response was significantly blunted in mice challenged with an irrelevant hapten, or by inhibition of effector cell recruitment, indicating a role for T cell–dependent inflammation in induction of Treg migration. Moreover, induction of Treg migration was inhibited by local injection of a CCR4 antagonist, indicating a role for CCR4 in this response. Exposure of naive mice to hapten also induced an increase in the proportion of migratory Tregs, demonstrating that innate signals can also induce Treg migration. Simultaneous examination of the migration of $CD4^+$ effector cells and Tregs in the same region of uninflamed skin demonstrated that effector cells behaved differently, being uniformly highly migratory. These findings indicate that Treg behavior in skin differs from that of $CD4^+$ effector cells, in that only a low proportion of Tregs is migratory under resting conditions. However, in response to both adaptive and innate inflammation, the proportion of migratory Tregs increases, raising the possibility that this response is important in multiple forms of skin inflammation. ***The Journal of Immunology*****, 2013, 191: 000–000.**

Regulatory T cells (Tregs) are a subset of $CD4^+$ T cells with a critical role in controlling inflammation in nonlymphoid tissues (1–4). A growing body of evidence suggests that Tregs must enter target organs to be effective in regulating inflammation in the periphery, indicating that many critical actions of Tregs occur in nonlymphoid tissues (5–8). Moreover, Tregs are found in many tissues under steady-state conditions, consistent with their ongoing presence in these sites being critical to tissue homeostasis (8, 9). Despite this, little is known regarding the actions of Tregs in the periphery.

Over the last decade, many insights into T cell biology have arisen from the use of in vivo multiphoton microscopy, although this work has primarily focused on effector T cell populations (10, 11). The multiphoton studies that have examined Tregs predominantly assessed their actions in lymph nodes (12, 13). These studies demonstrated that lymph node–resident Tregs are highly motile, an attribute that facilitates their interactions with numerous dendritic cells. Encountering a dendritic cell bearing its cognate Ag causes the Treg to prolong this interaction, a response associated with Treg-mediated suppression of effector cell priming. These behaviors are similar to those already described for effector T cells in the lymph node (10, 11). However, much less is known about the actions of Tregs in nonlymphoid tissues.

Multiphoton imaging studies demonstrated that effector T cells are constitutively migratory in the periphery, but alter their pattern of migration upon interaction with a cell bearing their cognate Ag (14–17). The nature of Treg behavior under similar circumstances is unknown. Some of the obstacles hindering analysis of endogenous Tregs have been their scarcity and lack of a surface-expressed marker distinguishing them from other $CD4^+$ T cell subsets. The Foxp3-GFP mouse, in which GFP is expressed exclusively in Tregs, overcomes this hurdle (18). We recently used intravital microscopy in these mice to detect endogenous Tregs adherent within the inflamed dermal microvasculature (19), although these studies did not extend to examination of extravascular Tregs. Recent studies used in vivo microscopy to demonstrate accumulation of both "natural" and induced Tregs in allografted pancreatic islets, as well as localization of Tregs in the bone marrow (20, 21). However, these studies did not examine Treg behavior in these nonlymphoid tissues. Therefore, the aim of these experiments was to use multiphoton microscopy to characterize the actions of Tregs in the periphery, both under resting conditions and during a T cell–driven inflammatory response. We found that in the absence of inflammation, tissue-resident Tregs were predominantly immotile, whereas following induction of inflammation via either adaptive or innate mechanisms, an increased proportion of Tregs was actively migrating throughout the dermis.

Materials and Methods

Mice

Eight- to ten-week-old male Foxp3-GFP mice, expressing GFP under the control of the Foxp3 promoter (C57BL/6 background) (18), were bred from

*Centre for Inflammatory Diseases, Monash University Department of Medicine, Monash Medical Centre, Clayton, Victoria 3168, Australia; and †Department of Microbiology and Immunology, The University of Melbourne, Melbourne, Victoria 3010, Australia

[1]J.A.D. and M.J.H. contributed equally to this work.

Received for publication November 20, 2012. Accepted for publication July 8, 2013.

This work was supported by funding from the National Health and Medical Research Council of Australia. M.J.H. is a National Health and Medical Research Council Senior Research Fellow.

Address correspondence and reprint requests to Dr. Michael Hickey, Centre for Inflammatory Diseases, Monash University Department of Medicine, Monash Medical Centre, 246 Clayton Road, Clayton, Victoria 3168, Australia. E-mail address: michael.hickey@monash.edu

The online version of this article contains supplemental material.

Abbreviations used in this article: CS, contact sensitivity; DNFB, 1-fluoro-2,4-dinitrobenzene; Oxa, oxazolone; PTx, pertussis toxin; Treg, regulatory T cell; TRITC, tetramethylrhodamine isothiocyanate.

stock generously provided by Dr. Alexander Rudensky (University of Washington, Seattle, WA, and Memorial Sloan–Kettering Cancer Center, New York, NY). All animal experiments were approved in advance by either the Monash Medical Centre Animal Ethics Committee "B" or the Melbourne Health Research Animal Ethics Committee.

Oxazolone-induced model of contact sensitivity

Contact sensitivity (CS) was induced as previously described (19, 22). Briefly, mice were sensitized by the application of 50 μl 5% oxazolone (4-ethoxymethylene-2-phenyl-2-oxazolin-5-one [Oxa]; Sigma-Aldrich, St. Louis, MO) in an acetone/olive oil vehicle (4:1) to a shaved region on the back. Five to seven days later, a 10 × 20-mm area of the flank was challenged with 1% Oxa in vehicle. In control experiments, mice sensitized in the same manner were challenged with vehicle alone or 0.2% 1-fluoro-2,4-dinitrobenzene (DNFB; Sigma-Aldrich) as an irrelevant hapten.

Multiphoton microscopy of the flank skin

Flank skin was prepared for multiphoton microscopy using a modification of a previously published technique (22). Mice were anesthetized (ketamine hydrochloride, 150 mg/kg; xylazine hydrochloride, 10 mg/kg), and a jugular vein was cannulated for administration of fluorescent dyes and additional anesthetic. A heating pad was used to maintain body temperature. The hair was removed from the challenged area of flank skin via brief treatment with depilatory cream. To ensure analysis of representative portions of all layers of the skin via multiphoton microscopy, the skin was imaged in two steps. The undersurface of the skin (hypodermis) was prepared for microscopy as previously described (19). Following imaging of the hypodermis, the skin preparation was inverted such that the epidermis was uppermost, and this region was imaged via multiphoton microscopy. To enable visualization of the vasculature, tetramethylrhodamine isothiocyanate (TRITC) albumin (375 μg/mouse) was administered i.v.

Skin multiphoton microscopy for both regions was performed with a Leica SP5 multiphoton confocal microscope equipped with a 20× 1.0 NA lens, four nondescanned detectors, and a Spectra-Physics Mai Tai laser. Experiments were performed at 900 nm excitation. Images (6 μm z step size) were collected to a depth of 100–125 μm and acquired every 30 s. Typical experiments involved four recordings of 5 min duration, from nonoverlapping regions in both hypodermis and dermis. In experiments in which Tregs and effector $CD4^+$ T cells were examined simultaneously or the effects of pertussis toxin (PTx) or CCR4 inhibitors were analyzed, recordings were of 25–30 min duration and were acquired every 60 s, at ∼2 μm z step size.

Image analysis

Treg abundance and migration were analyzed using Imaris (Bitplane, Zurich, Switzerland). Abundance was averaged from the four regions in the dermis and hypodermis and expressed as cells/mm^3. Migration was compared via analysis of displacement (μm) and mean velocity (μm/min). In some experiments, displacement was analyzed specifically in each of the X, Y, and Z planes.

Experimental protocol

Oxa-sensitized mice were examined via multiphoton microscopy at 4, 24, 48, and 72 h after Oxa challenge. As a control, sensitized mice were exposed to acetone/olive oil vehicle alone. To examine the effect of selectin blockade, RB40.34 (anti–P-selectin; 20 μg, BD Biosciences) and RME-1 (anti–E-selectin, 100 μg; generously provided by Dr. Andrew Issekutz, Dalhousie University, Halifax, NS, Canada) were administered i.v. 15 min before challenge (23). Control mice received the same amount of nonspecific IgG. To examine an Ag-independent model of inflammation, naive mice were exposed to 1% Oxa applied to the flank skin, exactly as for the sensitized mice, and examined 24 h later (24). To examine the role of chemoattractant receptors and CCR4 on Treg migration during CS, mice underwent sensitization and challenge as already described. Subsequently, anesthetized mice were injected intradermally with either PTx (List Biological Laboratories, Campbell, CA; 100 ng in PBS) or the CCR4 antagonist C 021 (R&D Systems; also known as *8ic*; 3 mg/kg in saline) (25) 20 h after CS challenge. Injections consisted of five 20-μl intradermal injections (total volume injected = 100 μl) in a 20 × 10-mm area on the challenged flank. Control mice were injected in a similar manner with saline. The injected region was imaged after an additional 4 h, as already described. To examine the role of mast cell degranulation on Treg migration, mice were treated with sodium cromoglycate (Sigma-Aldrich; 100 mg/kg/d, i.p) (26), starting 24 h prior to Oxa challenge, and examined via multiphoton imaging 24 h postchallenge.

Flow cytometric analysis of T cells in skin and lymph node

T cell recruitment to inflamed skin was quantitated using a modification of a previously described technique (19). In brief, skin samples were weighed, finely macerated, and dissociated using collagenase D (3 mg/ml) in RPMI 1640 plus 10% FCS and 0.1 mg/ml DNase (1 h, 37˚C). Dissociated skin was filtered through a 70-μm sieve, washed with RPMI/FCS, and labeled with cell surface Abs in PBS containing 1% FCS for 30 min on ice. Abs against cell surface molecules used were CD3 e450 (2 μg/ml; eBioscience, San Diego, CA), CD4 FITC (2.5 μg/ml; eBioscience), or CD4 PE (4 μg/ml; BD Biosciences) and CD45 PE Cy5.5 (2 μg/ml; eBioscience). To quantify the total number of T cells present, 25 μl CountBright counting beads (Life Technologies, Carlsbad, CA), containing a defined number of beads, was added to samples, allowing the proportion of the sample examined to be determined, and referenced to the number of T cells present in the same sample. Labeled cells were analyzed using a FACSCanto flow cytometer (BD Biosciences, North Ryde, NSW, Australia). In parallel, a sample of the same skin region was taken for wet weight/dry weight analysis. T cell recruitment data are expressed as $CD3^+/CD4^+$ cells/g of extrapolated skin dry weight. The numbers of Tregs present in lymph nodes were quantitated using a similar approach to analyze cells in macerated lymph nodes, in the absence of treatment with dissociation enzymes.

HSV-specific effector $CD4^+$ T cell model

Naive DsRed gDT-II $CD4^+$ T cells (1×10^5) were transferred into Foxp3-GFP mice, which subsequently underwent cutaneous HSV infection on the left flank, as previously described (17). Eight days later, skin on the contralateral uninfected flank was examined via multiphoton microscopy, as described (17).

Histology

Skin samples from Foxp3-GFP mice were immersion fixed in 4% paraformaldehyde, cryoprotected with 30% w/v sucrose in PBS, and frozen in Tissue-Tek OCT compound, and 8-μm cryostat sections were prepared. Sections were either stained with H&E or were stained with Hoechst 33258 to label nuclei for assessment of Treg location. The latter sections were visualized on a Nikon C1 confocal microscope. GFP^+ Tregs were counted and categorized according to their distance from the epidermis.

Statistics

Data were compared using one-way ANOVA and the Dunnett or Tukey post hoc test or using unpaired t tests. Data are shown as mean ± SEM. The p values < 0.05 were deemed significant.

Results

Skin-resident Tregs predominantly reside in the dermis

Because the ear is a commonly used site in the investigation of leukocyte function in skin, we first attempted to examine skin-resident Tregs via in vivo multiphoton microscopy of ear skin in Foxp3-GFP mice. However, GFP^+ cells were extremely rare and difficult to visualize at this site (data not shown). We recently examined Treg recruitment in a CS model involving abdominal flank skin and detected skin-resident Tregs in the absence of inflammation, as well as recruitment of additional Tregs during the inflammatory response (19). Therefore, we used multiphoton microscopy to examine this area of skin in Foxp3-GFP mice. Because multiphoton imaging was unable to penetrate all layers of the skin in this region, we visualized the dermis and hypodermis in separate procedures in the same mice, imaging the dermis via the external surface and the hypodermis via the exposed undersurface of the skin (22) (Fig. 1). In each case, we were able to visualize 100–125 μm into the tissue. The dermis was collagen rich and relatively avascular (Fig. 1B), whereas the hypodermis contained postcapillary venules supporting interacting leukocytes (Fig. 1C).

Tregs were rare in the hypodermis of uninflamed skin (Fig. 2A, 2C). In contrast, a consistently high number of Tregs was observed in the dermis (∼2000/mm^3) in the absence of inflammation (Fig. 2B, 2D). Intradermal Tregs were often observed in clusters around hair follicles (Fig. 1B). Flow cytometric analysis of T cells in dissociated skin samples confirmed that the GFP^+ cells in these

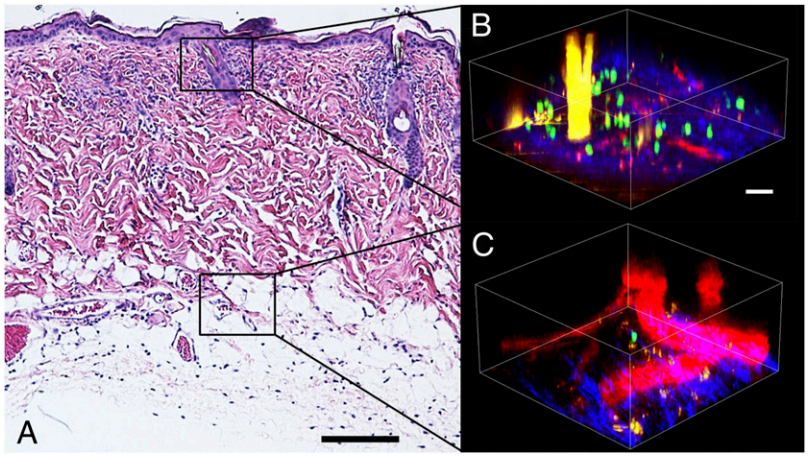

FIGURE 1. Multiphoton imaging approach for visualization of the dermis and hypodermis of flank skin. Diagram showing regions of flank skin examined when imaging either the hypodermis or the dermis. (**A**) Histological section of a typical skin sample stained with H&E. Scale bar, 200 μm. Three-dimensional renderings of the skin imaged via the external surface [dermis; (**B**)] or exteriorized undersurface [hypodermis; (**C**)] [scale bar in (B) and (C), 30 μm]. (C) In the hypodermis, the vasculature is readily visualized, via labeling with TRITC albumin (red), and Tregs (green) are infrequent. (B) In contrast, Tregs are present in greater numbers in the dermis. This layer is less vascular and also contains hair follicles (yellow), which are often surrounded by clusters of Tregs.

skin regions were CD4$^+$ T cells (data not shown). These data are consistent with our recent work and other studies reporting the presence of Tregs in uninflamed skin (8, 9, 19). Moreover, LysM-eGFP mice (in which neutrophils express GFP) that underwent an identical multiphoton imaging protocol displayed no neutrophil infiltration (data not shown), indicating that exteriorization and imaging the flank were not inducing inflammation that may have been responsible for recruitment of Tregs to the dermis.

Following induction of the CS response, a significant increase in Treg abundance in the hypodermis was observed 24 h after hapten challenge, persisting until ≥48 h (Fig. 2C). However, the number of Tregs in the hypodermis remained an order of magnitude lower than in the dermis. Occasional Tregs were also observed adherent within the hypodermal microvasculature (data not shown). Similarly, in the dermis, Treg abundance was significantly increased above basal levels 24 h after hapten challenge (Fig. 2D), although

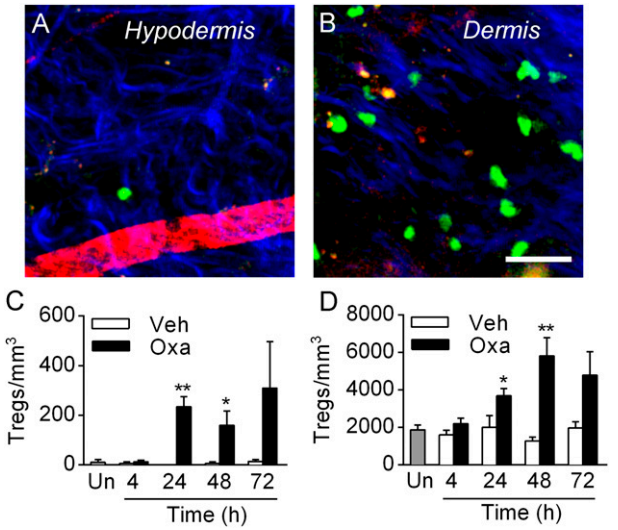

FIGURE 2. Skin-resident Tregs are predominantly in the dermis and increase in abundance during CS. Multiphoton images of hypodermis (**A**) and dermis (**B**) of a Foxp3-GFP mouse undergoing a CS response. The vasculature has been labeled with TRITC albumin (red), and collagen (blue) is detected via the second harmonic signal. Tregs (green) are more frequently observed in dermis versus hypodermis. Maximum projection images, Scale bar, 30 μm. Quantitation of Treg abundance in hypodermis (**C**) and dermis (**D**) in untreated mice (Un) and in sensitized mice following challenge with either vehicle alone (Veh) or Oxa. Data represent mean ± SEM of $n = 7$ untreated mice and $n = 6$–7 vehicle-challenged or Oxa-challenged mice at 4, 24, 48, and 72 h. *$p < 0.05$, **$p < 0.01$ versus vehicle-challenged mice at the time points shown.

no Tregs were observed within microvessels (data not shown). Together, these data indicate that, under resting and inflammatory conditions, Tregs are more numerous in the superficial dermis than in deeper layers of the skin.

Dermal Tregs and effector CD4$^+$ T cells display different patterns of migration in uninflamed skin

Given the relative abundance of Tregs in the uninflamed dermis, we next examined the migratory characteristics of Tregs in this region, in the absence of inflammation. To define a Treg as migratory, we established a threshold level of displacement of 10 μm, corresponding to cells that moved at least one cell width from their original position during the period of observation. In resting skin, Tregs were predominantly immotile, not moving from their original position (Fig. 3A–C, Supplemental Video 1). However, a small subset (7%) of the Tregs migrated >10 μm during the observation period (Fig. 3B). The immotile Tregs displayed occasional probing and elongation around their base position that resulted in measurement of an average velocity of ~4 μm/min (Fig. 3C). These observations indicate that dermal Tregs exist in two populations: one sessile and the other undergoing active migration.

These findings contrasted markedly with previous studies in which effector CD4$^+$ T cells in the dermis were uniformly highly migratory (17). It was conceivable that these divergent observations stemmed from differences between the inflammatory milieu in the two studies. Therefore, we next examined migration of Tregs and effector CD4$^+$ T cells in the same region of uninflamed skin. This was achieved by transferring naive HSV-specific gDT-II CD4$^+$ T cells into Foxp3-GFP mice and infecting one flank of the mouse with HSV. We then allowed 8 d for the HSV-specific T cells to undergo activation and subsequently migrate to the skin. At this point, examination of uninflamed skin remote from the site of HSV infection revealed that, as observed previously, effector CD4$^+$ T cells were uniformly highly motile (Fig. 3D, 3E, Supplemental Video 2). In fact, >90% of the gDT-II cells in these areas of uninflamed skin were defined as migratory. In contrast, Tregs in the same skin regions remained predominantly immotile (Fig. 3D, 3E, Supplemental Video 2). These findings demonstrate that Tregs and effector CD4$^+$ T cells display distinct migratory behavior in the skin.

Ag challenge induces migration of a subset of dermal Tregs

We next examined the effect of induction of T cell–dependent inflammation on the behavior of Tregs in the skin, concentrating on the more abundant dermal Tregs. Vehicle-treated control mice showed no significant changes in mean Treg displacement or velocity over a 72-h period (Fig. 4A, 4C, 4D). However, following oxazolone application to sensitized mice, Tregs gradually in-

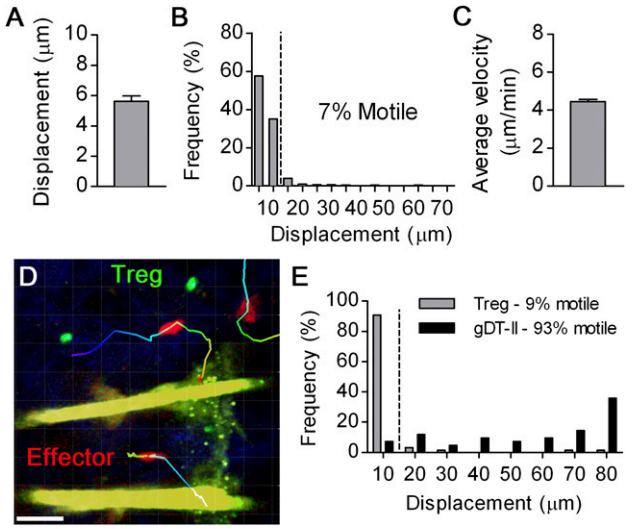

FIGURE 3. Dermal Tregs and effector cells display different migratory characteristics in the absence of inflammation. (**A**–**C**) Multiphoton assessment of Treg migration in dermis of uninflamed skin (see also Supplemental Video 1). (A) Mean Treg displacement during observation period. (B) Frequency distribution (%) of Treg displacement (in 5-μm intervals) in untreated mice. Dashed line indicates threshold (10 μm) above which cells were defined as motile. (C) Mean Treg velocity. Data in (A)–(C) were derived from n = 6–7 mice/group, incorporating 314 cells. Data in (A) and (C) represent mean ± SEM. (**D** and **E**) Comparison of Treg and effector $CD4^+$ T cell migration in same skin regions. (D) Multiphoton image of uninflamed dermis of Foxp3-GFP mouse containing GFP^+ Tregs (green) and DsRed-expressing gDT-II effector $CD4^+$ T cells (red). Tregs are immotile, whereas effector $CD4^+$ T cells are migratory (colored lines show paths of migration). Maximum projection image. Scale bar, 30 μm. See also Supplemental Video 2. (E) Frequency distribution (%) of displacement of Tregs and effector $CD4^+$ T cells (gDT-II) in the same regions of uninflamed dermis. Dashed line indicates threshold (10 μm) above which cells were defined as motile. Data were derived from analysis of 42 gDT-II and 64 Foxp3-GFP cells from n = 3 mice.

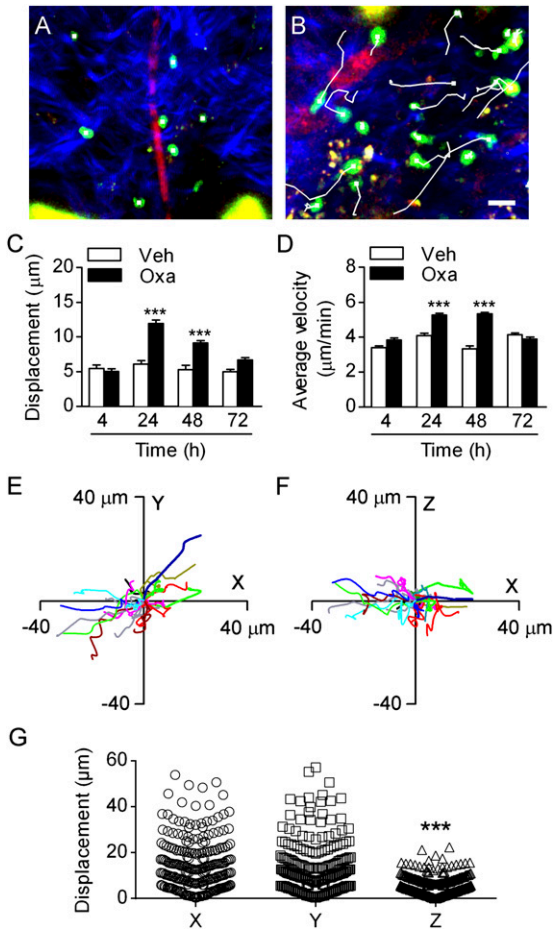

FIGURE 4. Ag challenge induces increased Treg migration. Images of hypodermis (**A**) and dermis (**B**) of Foxp3-GFP mice undergoing a CS response, with lines indicating paths of Treg migration in a 5-min observation period (see also Supplemental Video 3). Maximum projection images. Scale bar, 20 μm. Mean displacement (**C**) and migration velocity (**D**) of Tregs in dermis of sensitized mice 4, 24, 48, and 72 h after exposure to either vehicle (Veh) or Oxa. Data were derived from n = 6–7 mice/group, incorporating 150–300 cells/group (vehicle) or 280–740 cells/group (Oxa), and represent mean ± SEM. ***$p < 0.001$ versus vehicle-challenged mice at the time points shown. (**E**–**G**) Analysis of Treg migration in X, Y, and Z planes. (E and F) Three-dimensional depiction of dermal Treg migration in a sensitized mouse 24 h after Oxa challenge. Graphs show paths of individual migrating Tregs in the XY (E) and XZ (F) planes. Cell-migration paths are displayed as arising from a common point of origin. (G) Quantitative analysis of Treg migration during a CS response (24 h postchallenge), showing migratory displacement specifically in the X, Y, or Z plane. Data show results of analysis of 247 individual Tregs from six mice. ***$p < 0.001$ versus X and Y dimensions.

creased motility, displaying significantly increased displacement and migration velocity within 24 h of challenge, persisting out to 48 h postchallenge, relative to vehicle-treated controls (Fig. 4B–D, Supplemental Video 3). Assessment of the directionality of Treg migration at the peak of the response (24 h post-Oxa challenge) demonstrated that migrating Tregs moved randomly in the XY plane but were confined to a 50-μm-thick zone of the dermis, as determined by assessment of migration in the XZ plane (Fig. 4E, 4F). This was further demonstrated by comparison of the displacement of migrating Tregs specifically in each of the X, Y, and Z planes. Displacement in X (14.2 ± 0.7 μm) and Y (13.3 ± 0.7 μm) planes were comparable, whereas migration in the Z plane (5.7 ± 0.3 μm) was significantly lower (Fig. 4G).

We next examined the effect of CS challenge on the proportion of migratory Tregs and found that, 4 h after initiation of CS, there was no change in this parameter relative to vehicle-challenged mice (Fig. 5A, 5B). In contrast, 24 h after CS challenge, 40% of Tregs were migratory compared with 16% in vehicle-treated mice (Fig. 5C, 5D). Notably, despite the difference in the relative proportions of migratory Tregs under these conditions, assessment of the migratory subsets separately demonstrated that the average velocity of migratory Tregs during the CS response did not differ from that in the absence of treatment (untreated: 8.4 ± 0.6 μm/s, n = 23; CS/24 h: 7.3 ± 0.1 μm/s, n = 249). This finding indicates that the measured increase in average migration velocity stemmed solely from an increase in the proportion of migrating Tregs. The increase in the proportion of migratory Tregs persisted 48 h after challenge (Fig. 5E, 5F), consistent with the observed significant increase in mean velocity (Fig. 4D).

Ag recognition and leukocyte recruitment contribute to induction of Treg migration

We next investigated the role of Ag recognition and leukocyte recruitment in induction of Treg migration. To assess whether increased Treg migration was a downstream response to recognition of the sensitizing Ag upon challenge, mice were sensitized to Oxa and then challenged either with Oxa or an irrelevant hapten (DNFB) (Fig. 6). Twenty-four hours after challenge, the numbers of Tregs in the hypodermis and the dermis were both significantly reduced in DNFB-challenged mice relative to Oxa-challenged mice (Fig. 6A, 6B), findings consistent with Treg recruitment during the

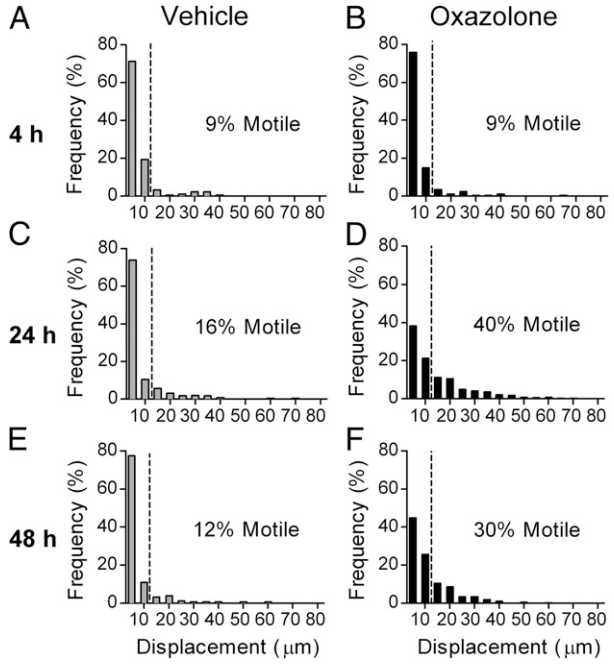

FIGURE 5. A subset of dermal Tregs increases migration during CS. Frequency distributions (%) of Treg displacement in sensitized mice 4 h (**A**, **B**), 24 h (**C**, **D**), and 48 h (**E**, **F**) after challenge with vehicle (A, C, E) or oxazolone (B, D, F). Dashed lines indicate threshold (10 μm) above which cells were defined as motile. Data were derived from $n = 6–7$ mice/group, incorporating 150–300 cells/group (vehicle) or 280–740 cells/group (Oxa).

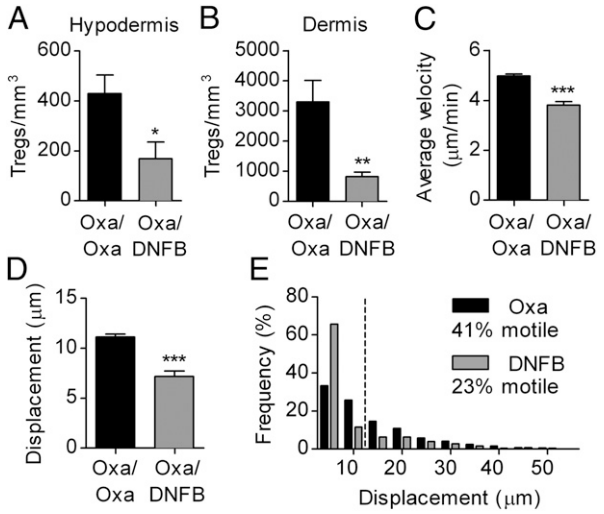

FIGURE 6. Adaptive mechanisms contribute to induction of Treg recruitment and migration in CS. Mice underwent Oxa sensitization and were subsequently challenged with either oxazolone (Oxa/Oxa) or the alternate hapten DNFB (Oxa/DNFB), and Treg abundance and migration were examined after 24 h via multiphoton microscopy. Data are shown for Treg abundance in hypodermis (**A**) and dermis (**B**), as well as mean velocity (**C**) and displacement (**D**) of dermal Tregs. (**E**) Frequency distribution (%) of Treg displacement in both groups. Dashed line indicates threshold (10 μm) above which cells were defined as motile. Data represent analysis >250 cells derived from 12 mice/group and are shown as mean ± SEM. $*p < 0.05$, $**p < 0.01$, $***p < 0.001$ versus Oxa/Oxa group.

CS response being driven by a recall response to the sensitizing hapten. In addition, the average Treg migration velocity (Fig. 6C) and displacement (Fig. 6D) were significantly lower in DNFB-challenged mice relative to mice challenged with Oxa. These findings stemmed from a reduction in the proportion of migratory Tregs in DNFB-challenged mice (Fig. 6E). These data are consistent with the concept that induction of Treg migration during CS is mediated in part via Ag recognition via the adaptive immune system.

As a further way of assessing the role of the adaptive immune response in induction of Treg migration, we next examined the effect of inhibiting dermal leukocyte recruitment during the early phase of the response. Hwang et al. (27) showed that prevention of $CD4^+$ effector T cell recruitment during the first 2 h of the challenge phase, via inhibition of endothelial adhesion molecules P- and E-selectin, was sufficient to prevent CS-associated inflammation. Therefore, we asked whether a similar strategy might alter the CS-associated increase in Treg migration. Sensitized mice were administered function-blocking Abs against P- and E-selectin shortly before Oxa challenge. Mice that received selectin-blocking Abs displayed a small but significant reduction in edema, and significantly reduced $CD4^+$ T cell recruitment at 24 h (Fig. 7A, 7B), demonstrating that this treatment inhibited the inflammatory response to some extent. In line with this finding, Treg recruitment to the inflamed dermis was reduced relative to CS mice that received control Ab (Fig. 7C). Assessment of the migration of the Treg population remaining in the dermis in anti-selectin Ab–treated mice revealed that mean Treg displacement (Fig. 7D) was significantly reduced relative to control Ab-treated mice, an effect associated with a reduction in the proportion of motile cells relative to control Ab–treated mice (Fig. 7E). In addition, the mean velocity of Tregs was slightly, but significantly, lower in selectin-inhibited mice (Fig. 7F). These data indicate that selectin-mediated leukocyte recruitment during the effector phase contributes to some degree to induction of Treg migration in this model of CS. However, the small magnitude of the effect of selectin inhibition indicates that other inflammatory mechanisms contribute to a greater extent.

Migration of dermal Tregs is reduced by CCR4 inhibition

We next assessed the role of chemoattractant pathways in induction of Treg migration. First, we used PTx as a tool to block chemoattractant receptor–dependent signaling in Tregs. PTx was injected intradermally, 20 h after induction of CS, allowing time for recruitment of leukocytes, including Tregs, into the skin as part of the normal CS response. Treg migration was then examined by multiphoton microscopy after an additional 4 h, 24 h after CS challenge, using 30-min recordings at 60-s intervals to increase the precision of the analysis (Fig. 8). In mice injected with PTx, Treg displacement and average velocity were significantly reduced relative to CS mice injected intradermally with saline (Fig. 8).

Given that CCR4 has been shown to play a key role in Treg homing to the skin (8), we next examined the role of CCR4 in CS-associated Treg migration. Using a similar approach to the PTx experiments, we injected C 021, a small molecule CCR4 inhibitor (25) intradermally, 20 h after Oxa challenge, and examined Treg migration after an additional 4 h. CCR4 inhibition resulted in significant reductions in Treg displacement and average velocity (Fig. 8, Supplemental Videos 4, 5). In addition, the percentage of motile cells (displacement > 10 μm) decreased from 47% in saline-injected mice to 25 and 27% in PTx- and C 021-treated mice, respectively. Together, these results indicate that a CCR4-dependent mechanism plays a key role in induction of intradermal Treg migration in CS.

To determine whether mast cell activation contributed to this response, we also examined Treg migration in CS mice treated with the mast cell stabilizer, sodium cromoglycate (cromolyn). In cromolyn-treated mice, Treg migration parameters did not differ from those in control mice (data not shown), indicating that mast cell degranulation was not required for induction of Treg migration in this response.

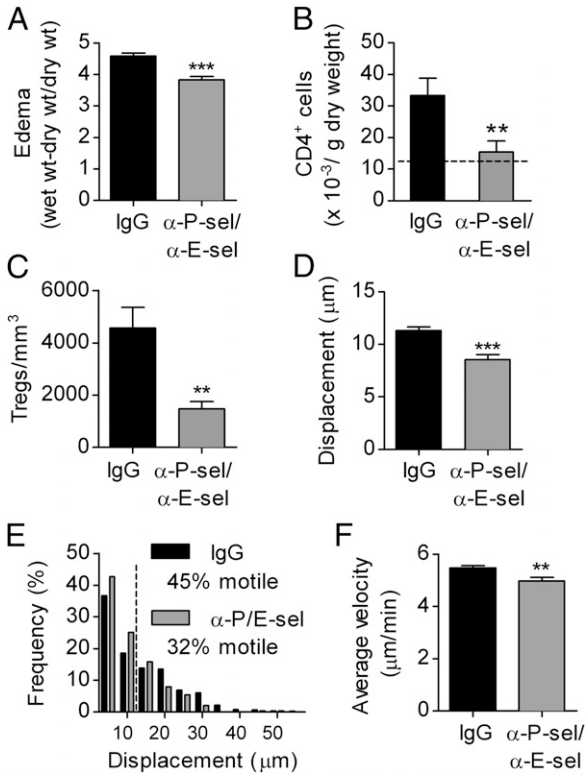

FIGURE 7. Selectin inhibition reduces induction of Treg migration. Effect of inhibition of P-selectin and E-selectin during the challenge phase of the CS response. Mice received either anti–P-selectin/anti–E-selectin (α–P-sel/α–E-sel) or control Ab (IgG) at the start of the challenge phase and were examined 24 h later. Data are shown for skin edema (**A**); number of $CD3^+/CD4^+$ cells in the challenged region of skin, as determined using flow cytometric analysis of dissociated skin (**B**; dashed line indicates Treg abundance in vehicle-challenged skin); and Treg abundance in dermis (**C**), as determined by multiphoton microscopy. (**D**–**F**) Effect of selectin inhibition on Treg migration. (D) Mean Treg displacement. (E) Frequency (%) of Treg displacement in anti-selectin Ab-treated versus control IgG–treated mice (dashed line indicates 10 μm threshold above which cells were defined as motile). (F) Mean Treg velocity. Data represent analysis of >239 cells derived from $n = 6$ mice/group and are shown as mean ± SEM. $^{**}p < 0.01$, $^{***}p < 0.001$ versus IgG group.

Dermal Tregs respond to a local innate stimulus

Finally, it was notable that following challenge with an irrelevant hapten, as well as in mice in which CS-associated effector leukocyte recruitment was inhibited, Treg migration remained above levels observed in uninflamed skin. One possible explanation for this observation is that dermal hapten exposure alone was sufficient to induce Treg migration. Haptens are capable of causing inflammation in nonsensitized animals, demonstrating their capacity to induce innate responses (17, 24, 28). Therefore, we next assessed whether dermal exposure to Oxa was capable of inducing Treg migration in the absence of prior sensitization. Unexpectedly, 24 h after exposure of naive mice to 1% Oxa, Treg numbers (as detected via multiphoton imaging) were unaltered in the hypodermis, but were significantly reduced in the dermis, relative to untreated mice (Supplemental Fig. 1A, 1B). In contrast to this finding, flow cytometric analysis of the Treg content of the full-thickness skin and draining lymph nodes showed no significant alteration in Treg abundance in either location (Supplemental Fig. 1C, 1D), indicating that Tregs were not migrating from the skin to the draining lymph nodes. However, histological analysis of skin sections demonstrated that hapten-exposed skin was significantly swollen (Supplemental Fig. 1E–G), and the proportion of skin-resident Tregs (detected via GFP expression) present in the outermost ~ 125 μm accessible to multiphoton microscopy was significantly reduced relative to that in untreated skin (Supplemental Fig. 1H–J). The latter findings explain the reduction in dermal Tregs detected via multiphoton imaging (Supplemental Fig. 1B).

In Oxa-treated mice, analysis of migration of the dermal Tregs detectable via multiphoton imaging revealed that displacement was significantly increased above that in untreated controls (Fig. 9A). As seen in CS, this increase stemmed from an increase in the proportion of motile cells (Fig. 9B) above the level in untreated skin (7%, Fig. 3B). These experiments reveal that dermal Treg behavior can also be modulated by an innate inflammatory stimulus.

Discussion

Despite studies demonstrating that Tregs must home to peripheral organs to provide effective regulation of local inflammation (5–8), the actions of Tregs in these sites are poorly understood. In this study, we show that, under both resting and inflammatory conditions, skin-resident Tregs exist in two populations: nonmotile or actively migrating throughout the dermis. In the absence of inflammation, the migratory population represents <10% of Tregs. However, upon inflammatory stimulation, the proportion of migratory Tregs increases. Interestingly, this response occurs to varying degrees both upon exposure of sensitized mice to the sensitizing

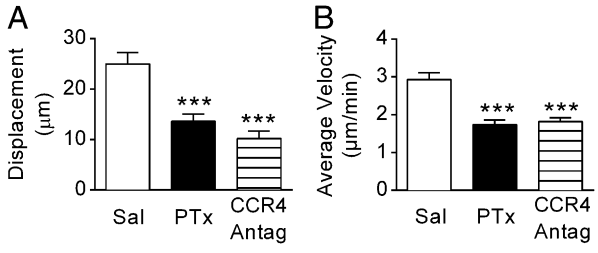

FIGURE 8. CS-associated Treg migration is reduced via CCR4 inhibition. Effect of PTx and CCR4 inhibition on Treg migration during CS. Mice underwent sensitization and Oxa challenge; 20 h after challenge, they were injected intradermally with saline (Sal) as control, PTx, or the CCR4 antagonist, C 021 (see also Supplemental Videos 4, 5). Treg migration was examined by multiphoton microscopy after an additional 4 h, 24 h after challenge. Data are shown for Treg displacement (**A**) and average Treg velocity (**B**). Data represent analysis of $n = 6$ mice/group and 189, 249, and 95 cells for saline, PTx, or CCR4 antagonist, respectively. $^{***}p < 0.001$ versus saline-injected group.

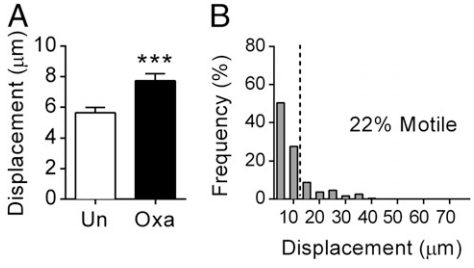

FIGURE 9. Innate inflammation induces alterations in dermal Treg migration. Oxa (1%) was applied to the skin of naive Foxp3-GFP mice, and Treg migration was examined 24 h later (Oxa). Data were compared with those from a group of untreated mice examined in parallel. (**A**) Mean Treg displacement in untreated (Un) and Oxa-treated mice. (**B**) Frequency distribution (%) of displacement of dermal Tregs 24 h after Oxa exposure in nonsensitized mice. Dashed line indicates threshold (10 μm) above which cells were defined as motile. Data represent analysis >230 cells from n = 5–7 mice/group and are shown as mean ± SEM. $^{***}p < 0.001$ versus untreated mice.

Ag and in nonsensitized mice in response to an innate inflammatory stimulus. This suggests that increased Treg migration is a fundamental component of the response of skin to inflammatory stimulation.

Although Tregs have been shown to be important in suppression of inflammation in this model of CS, the role of increased Treg motility in Treg-mediated suppression of inflammation is unknown (29). One hypothesis to explain the anti-inflammatory effects of Tregs is that this occurs via bystander suppression, as a result of nondirected release of broadly acting anti-inflammatory mediators (1, 2). It is conceivable that induction of Treg migration allows soluble mediators released by Tregs to affect a greater expanse of tissue, potentially achieving a more effective bystander suppression effect. This behavior may also increase the probability of Tregs encountering other immune cells with roles in skin inflammation. The finding that the majority of Tregs are sessile in uninflamed skin may indicate that these putative functions are minimally required in the absence of an overt inflammatory stimulus.

Previous studies demonstrated that Tregs represent a substantial proportion of the $CD4^+$ T cell population that undergoes constitutive migration from the skin to the draining lymph node under steady-state conditions (30). These findings are somewhat difficult to reconcile with the present finding that only a small proportion of the dermal Tregs are actively migratory. Recent studies in humans and mice provide evidence that the skin is a major reservoir of nonrecirculating, resident effector memory T cells (9, 31–33). These resident cells are thought to serve important functions in controlling local immune responses. Given the present findings, it is conceivable that the sessile Tregs make up the major Treg population that is resident in the skin, whereas the migratory Tregs may represent a subpopulation of cells, potentially of a different phenotype, which are in the process of trafficking to the local lymph nodes (30). It will be important to determine whether the migratory Tregs are recent immigrants into the skin or resident cells that have been stimulated to mobilize.

The finding that Oxa induced Treg migration in nonsensitized animals (i.e., via an innate pathway) suggests that an element of the innate response to this irritant is sufficient for induction of Treg migration. This is supported by recent observations of induction of Treg migration in the skin of naive mice within 5–20 min following intradermal infection with malaria sporozoites (34). Hapten exposure has been shown to induce activation of an innate inflammatory response via pathways including release of danger-associated molecular patterns and pattern recognition receptor activation (28). Responses of this nature have the potential to induce release of numerous inflammatory mediators that could modulate Treg migration. In support of this concept, a recent study provided evidence that the actions of Tregs were critical in suppression of MyD88-mediated inflammatory responses in organs such as the skin and gut, where commensal micro-organisms provide tonic inflammatory stimulation (35). This provides evidence that Tregs in organs at environmental interfaces act to limit inflammation initiated by innate inflammatory activation. The present findings, in which Treg migration was induced by an innate stimulus, may represent a previously unappreciated aspect of this important Treg response.

Despite the fact that we observed an alteration in Treg migration in response to an innate stimulus, the Treg migration response induced following re-exposure to sensitizing Ag was substantially more robust and resulted in recruitment of additional Tregs. Our studies using an alternative hapten in the challenge phase indicate that Ag recognition by the adaptive immune system contributed to the increase in Treg migration. Limiting leukocyte recruitment during the effector phase also resulted in a reduction in the extent of alteration in Treg migration. Although these studies emphasize the importance of the recognition of the hapten by the adaptive immune system, they do not demonstrate that the Tregs are responding via Ag recognition. Subtracting the proportion of Tregs migrating in response to cognate Ag exposure (Oxa, 41%) from that of Tregs migrating in sensitized mice in response to an irrelevant hapten (DNFB, 23%) indicates that Ag recognition contributes to altered migration ~18% of skin Tregs. It is conceivable, but unlikely, that 18% of the dermal Tregs in sensitized mice are specific for Oxa. An alternative explanation is that Ag recognition drives induction of inflammation; subsequently, the proportion of Tregs induced to undergo migration is relative to the intensity of the inflammatory response, with the Ag-induced inflammation being more intense than the innate response to Oxa.

Treg migration during CS was sensitive to inhibition by PTx, implicating $G\alpha_1$-coupled chemoattractant receptors in mediating this response. Given the key role of CCR4 in Treg homing to the skin, we reasoned that CCR4 would be a logical candidate receptor responsible for this migration (8). Experiments with a CCR4 antagonist supported this hypothesis, in that CCR4 inhibition resulted in a reduction in Treg migration comparable to that induced by PTx. Identification of CCR4 as critical to this response invokes roles for one or both of the CCR4 ligands, CCL17 and CCL22, in CS-associated Treg migration. Both CCL17 and CCL22 are produced by activated dendritic cells and have been shown to facilitate recruitment of T cells to the skin (8, 36). The present findings raise the possibility that these chemoattractants also modulate the actions of Tregs present in the skin, although this hypothesis will require further investigation. Notably, recent studies show that the absence of CCR4 exacerbates Oxa-induced CS, indicating that the major effect mediated by CCR4-dependent signaling in this model is regulation of inflammation (37). The present findings raise the possibility that CCR4-dependent Treg migration may contribute to this regulatory response.

In addition to investigating Treg migration, these experiments examined the compartmentalization of Tregs within the skin; they were abundant in the dermis, whereas they were relatively scarce in the deeper layers. Because the dermis is more likely to be exposed to inflammatory stimuli from the external environment, it is possible that the inflammation-suppressing actions of Tregs are more critical in this region. However, it was notable that induction of CS resulted in increased numbers of Tregs in the hypodermis. In addition, Tregs were observed undergoing intravascular adhesion in vessels in the hypodermis but not in the more superficial layers. Because adhesion is required for delivery of circulating leukocytes to sites of inflammation, these findings led us to speculate that the hypodermal vasculature is an important route of delivery of Tregs into the inflamed skin and that, upon exiting the vasculature in this location, Tregs subsequently migrate to the more superficial dermis. More work is required to determine the validity of this hypothesis. An additional consideration emerging from the analysis of Treg compartmentalization in the skin in these experiments is that inflammation-associated swelling impacts on the capacity of multiphoton imaging to detect intradermal Tregs. This observation illustrates that experiments using imaging to examine Treg recruitment to the inflamed skin need to be supported by alternative approaches, such as histology and flow cytometry, as we did in this study and previously (19).

In conclusion, these data indicate that increased Treg migration is an inherent element of the response of the skin to inflammation. Indeed, it is notable that the number of Tregs stimulated to undergo this response was proportional to the level of inflammation affecting the skin. Although it is tempting to speculate that induction of migration is indicative of activation of Treg suppressor function, it remains unclear whether this migration is critical to the ability

of Tregs to limit dermal inflammation. Future studies will aim to determine whether this behavior contributes to Treg-mediated suppression of skin inflammation.

Acknowledgments

We thank Dr. Alexander Rudensky for provision of Foxp3-GFP mice, Dr. Andrew Issekutz for provision of RME-1, Dr. Camden Lo (Monash Micro Imaging, Monash University) for assistance with image analysis, and the Monash Institute of Medical Research histology service for assistance with histology.

Disclosures

The authors have no financial conflicts of interest.

References

1. Tang, Q., and J. A. Bluestone. 2008. The Foxp3+ regulatory T cell: a jack of all trades, master of regulation. *Nat. Immunol.* 9: 239–244.
2. Vignali, D. A., L. W. Collison, and C. J. Workman. 2008. How regulatory T cells work. *Nat. Rev. Immunol.* 8: 523–532.
3. Bennett, C. L., J. Christie, F. Ramsdell, M. E. Brunkow, P. J. Ferguson, L. Whitesell, T. E. Kelly, F. T. Saulsbury, P. F. Chance, and H. D. Ochs. 2001. The immune dysregulation, polyendocrinopathy, enteropathy, X-linked syndrome (IPEX) is caused by mutations of FOXP3. *Nat. Genet.* 27: 20–21.
4. Brunkow, M. E., E. W. Jeffery, K. A. Hjerrild, B. Paeper, L. B. Clark, S. A. Yasayko, J. E. Wilkinson, D. Galas, S. F. Ziegler, and F. Ramsdell. 2001. Disruption of a new forkhead/winged-helix protein, scurfin, results in the fatal lymphoproliferative disorder of the scurfy mouse. *Nat. Genet.* 27: 68–73.
5. Siegmund, K., M. Feuerer, C. Siewert, S. Ghani, U. Haubold, A. Dankof, V. Krenn, M. P. Schön, A. Scheffold, J. B. Lowe, et al. 2005. Migration matters: regulatory T-cell compartmentalization determines suppressive activity in vivo. *Blood* 106: 3097–3104.
6. Suffia, I., S. K. Reckling, G. Salay, and Y. Belkaid. 2005. A role for CD103 in the retention of CD4+CD25+ Treg and control of *Leishmania major* infection. *J. Immunol.* 174: 5444–5455.
7. Yurchenko, E., M. Tritt, V. Hay, E. M. Shevach, Y. Belkaid, and C. A. Piccirillo. 2006. CCR5-dependent homing of naturally occurring CD4+ regulatory T cells to sites of *Leishmania major* infection favors pathogen persistence. *J. Exp. Med.* 203: 2451–2460.
8. Sather, B. D., P. Treuting, N. Perdue, M. Miazgowicz, J. D. Fontenot, A. Y. Rudensky, and D. J. Campbell. 2007. Altering the distribution of Foxp3(+) regulatory T cells results in tissue-specific inflammatory disease. *J. Exp. Med.* 204: 1335–1347.
9. Clark, R. A., B. Chong, N. Mirchandani, N. K. Brinster, K. Yamanaka, R. K. Dowgiert, and T. S. Kupper. 2006. The vast majority of CLA+ T cells are resident in normal skin. *J. Immunol.* 176: 4431–4439.
10. Mempel, T. R., S. E. Henrickson, and U. H. Von Andrian. 2004. T-cell priming by dendritic cells in lymph nodes occurs in three distinct phases. *Nature* 427: 154–159.
11. Cahalan, M. D., and I. Parker. 2008. Choreography of cell motility and interaction dynamics imaged by two-photon microscopy in lymphoid organs. *Annu. Rev. Immunol.* 26: 585–626.
12. Tang, Q., J. Y. Adams, A. J. Tooley, M. Bi, B. T. Fife, P. Serra, P. Santamaria, R. M. Locksley, M. F. Krummel, and J. A. Bluestone. 2006. Visualizing regulatory T cell control of autoimmune responses in nonobese diabetic mice. *Nat. Immunol.* 7: 83–92.
13. Mempel, T. R., M. J. Pittet, K. Khazaie, W. Weninger, R. Weissleder, H. von Boehmer, and U. H. von Andrian. 2006. Regulatory T cells reversibly suppress cytotoxic T cell function independent of effector differentiation. *Immunity* 25: 129–141.
14. Kawakami, N., U. V. Nägerl, F. Odoardi, T. Bonhoeffer, H. Wekerle, and A. Flügel. 2005. Live imaging of effector cell trafficking and autoantigen recognition within the unfolding autoimmune encephalomyelitis lesion. *J. Exp. Med.* 201: 1805–1814.
15. Mrass, P., H. Takano, L. G. Ng, S. Daxini, M. O. Lasaro, A. Iparraguirre, L. L. Cavanagh, U. H. von Andrian, H. C. Ertl, P. G. Haydon, and W. Weninger. 2006. Random migration precedes stable target cell interactions of tumor-infiltrating T cells. *J. Exp. Med.* 203: 2749–2761.
16. Matheu, M. P., C. Beeton, A. Garcia, V. Chi, S. Rangaraju, O. Safrina, K. Monaghan, M. I. Uemura, D. Li, S. Pal, et al. 2008. Imaging of effector memory T cells during a delayed-type hypersensitivity reaction and suppression by Kv1.3 channel block. *Immunity* 29: 602–614.
17. Gebhardt, T., P. G. Whitney, A. Zaid, L. K. Mackay, A. G. Brooks, W. R. Heath, F. R. Carbone, and S. N. Mueller. 2011. Different patterns of peripheral migration by memory CD4+ and CD8+ T cells. *Nature* 477: 216–219.
18. Fontenot, J. D., J. P. Rasmussen, L. M. Williams, J. L. Dooley, A. G. Farr, and A. Y. Rudensky. 2005. Regulatory T cell lineage specification by the forkhead transcription factor foxp3. *Immunity* 22: 329–341.
19. Deane, J. A., L. D. Abeynaike, M. U. Norman, J. L. Wee, A. R. Kitching, P. Kubes, and M. J. Hickey. 2012. Endogenous regulatory T cells adhere in inflamed dermal vessels via ICAM-1: association with regulation of effector leukocyte adhesion. *J. Immunol.* 188: 2179–2188.
20. Fan, Z., J. A. Spencer, Y. Lu, C. M. Pitsillides, G. Singh, P. Kim, S. H. Yun, V. Toxavidis, T. B. Strom, C. P. Lin, and M. Koulmanda. 2010. In vivo tracking of 'color-coded' effector, natural and induced regulatory T cells in the allograft response. *Nat. Med.* 16: 718–722.
21. Fujisaki, J., J. Wu, A. L. Carlson, L. Silberstein, P. Putheti, R. Larocca, W. Gao, T. I. Saito, C. Lo Celso, H. Tsuyuzaki, et al. 2011. In vivo imaging of Treg cells providing immune privilege to the haematopoietic stem-cell niche. *Nature* 474: 216–219.
22. Norman, M. U., S. Hulliger, P. Colarusso, and P. Kubes. 2008. Multichannel fluorescence spinning disk microscopy reveals early endogenous CD4 T cell recruitment in contact sensitivity via complement. *J. Immunol.* 180: 510–521.
23. Norman, M. U., N. Van De Velde, J. R. Timoshanko, A. Issekutz, and M. J. Hickey. 2003. Overlapping roles of endothelial selectins and VCAM-1 in immune complex-induced leukocyte recruitment in the cremasteric microvasculature. *Am. J. Pathol.* 163: 1491–1503.
24. Dudeck, A., J. Dudeck, J. Scholten, A. Petzold, S. Surianarayanan, A. Köhler, K. Peschke, D. Vöhringer, C. Waskow, T. Krieg, et al. 2011. Mast cells are key promoters of contact allergy that mediate the adjuvant effects of haptens. *Immunity* 34: 973–984.
25. Yokoyama, K., N. Ishikawa, S. Igarashi, N. Kawano, N. Masuda, W. Hamaguchi, S. Yamasaki, Y. Koganemaru, K. Hattori, T. Miyazaki, et al. 2009. Potent and orally bioavailable CCR4 antagonists: Synthesis and structure-activity relationship study of 2-aminoquinazolines. *Bioorg. Med. Chem.* 17: 64–73.
26. Ramos, L., G. Peña, B. Cai, E. A. Deitch, and L. Ulloa. 2010. Mast cell stabilization improves survival by preventing apoptosis in sepsis. *J. Immunol.* 185: 709–716.
27. Hwang, J. M., J. Yamanouchi, P. Santamaria, and P. Kubes. 2004. A critical temporal window for selectin-dependent CD4+ lymphocyte homing and initiation of late-phase inflammation in contact sensitivity. *J. Exp. Med.* 199: 1223–1234.
28. Kaplan, D. H., B. Z. Igyártó, and A. A. Gaspari. 2012. Early immune events in the induction of allergic contact dermatitis. *Nat. Rev. Immunol.* 12: 114–124.
29. Lehtimaki, S., T. Savinko, K. Lahl, T. Sparwasser, H. Wolff, A. Lauerma, H. Alenius, and N. Fyhrquist. 2012. The temporal and spatial dynamics of Foxp3+ Treg cell-mediated suppression during contact hypersensitivity responses in a murine model. *J. Invest. Dermatol.* 132: 2744–2751.
30. Tomura, M., T. Honda, H. Tanizaki, A. Otsuka, G. Egawa, Y. Tokura, H. Waldmann, S. Hori, J. G. Cyster, T. Watanabe, et al. 2010. Activated regulatory T cells are the major T cell type emigrating from the skin during a cutaneous immune response in mice. *J. Clin. Invest.* 120: 883–893.
31. Gebhardt, T., L. M. Wakim, L. Eidsmo, P. C. Reading, W. R. Heath, and F. R. Carbone. 2009. Memory T cells in nonlymphoid tissue that provide enhanced local immunity during infection with herpes simplex virus. *Nat. Immunol.* 10: 524–530.
32. Jiang, X., R. A. Clark, L. Liu, A. J. Wagers, R. C. Fuhlbrigge, and T. S. Kupper. 2012. Skin infection generates non-migratory memory CD8+ T(RM) cells providing global skin immunity. *Nature* 483: 227–231.
33. Clark, R. A., R. Watanabe, J. E. Teague, C. Schlapbach, M. C. Tawa, N. Adams, A. A. Dorosario, K. S. Chaney, C. S. Cutler, N. R. Leboeuf, et al. 2012. Skin effector memory T cells do not recirculate and provide immune protection in alemtuzumab-treated CTCL patients. *Sci. Transl. Med.* 4: 117ra7.
34. da Silva, H. B., S. S. Caetano, I. Monteiro, I. Gómez-Conde, K. Hanson, C. Penha-Gonçalves, D. N. Olivieri, M. M. Mota, C. R. Marinho, M. R. D'Imperio Lima, and C. E. Tadokoro. 2012. Early skin immunological disturbance after *Plasmodium*-infected mosquito bites. *Cell. Immunol.* 277: 22–32.
35. Rivas, M. N., Y. T. Koh, A. Chen, A. Nguyen, Y. H. Lee, G. Lawson, and T. A. Chatila. 2012. MyD88 is critically involved in immune tolerance breakdown at environmental interfaces of Foxp3-deficient mice. *J. Clin. Invest.* 122: 1933–1947.
36. Wang, X., M. Fujita, R. Prado, A. Tousson, H. C. Hsu, A. Schottelius, D. R. Kelly, P. A. Yang, Q. Wu, J. Chen, et al. 2010. Visualizing CD4 T-cell migration into inflamed skin and its inhibition by CCR4/CCR10 blockades using in vivo imaging model. *Br. J. Dermatol.* 162: 487–496.
37. Lehtimäki, S., S. Tillander, A. Puustinen, S. Matikainen, T. Nyman, N. Fyhrquist, T. Savinko, M. L. Majuri, H. Wolff, H. Alenius, and A. Lauerma. 2010. Absence of CCR4 exacerbates skin inflammation in an oxazolone-induced contact hypersensitivity model. *J. Invest. Dermatol.* 130: 2743–2751.